Pristine quantum criticality in a Kondo semimetal

W. T. Fuhrman[1,⊕,†], A. Sidorenko[2,⊕], J. Hänel[2], H. Winkler[2], A. Prokofiev[2], J. A. Rodriguez-Rivera[3,4], Y. Qiu[4], P. Blaha[5], Q. Si[6], C. L. Broholm[1,4,7], and S. Paschen[2,6,*]

[1]Institute for Quantum Matter and Department of Physics and Astronomy, The Johns Hopkins University, Baltimore, Maryland 21218 USA

[2]Institute of Solid State Physics, Vienna University of Technology, Wiedner Hauptstr. 8-10, 1040 Vienna, Austria

[3]Department of Materials Sciences, University of Maryland, College Park, Maryland 20742, USA

[4]NIST Center for Neutron Research, National Institute of Standards and Technology, Gaithersburg, MD 20899, USA

[5]Institute of Materials Chemistry, Vienna University of Technology, 1040 Vienna, Austria

[6]Department of Physics and Astronomy, Rice Center for Quantum Materials, Rice University, Houston, Texas 77005, USA

[7]Department of Materials Science and Engineering, The Johns Hopkins University, Baltimore, Maryland 21218 USA

The observation of quantum criticality in diverse classes of strongly correlated electron systems has been instrumental in establishing ordering principles, discovering new phases, and identifying the relevant degrees of freedom and interactions. At focus so far have been insulators and metals. Semimetals, which are of great current interest as candidate phases with nontrivial topology, are much less explored in experiments. Here we study the Kondo semimetal $CeRu_4Sn_6$ by magnetic susceptibility, specific heat, and inelastic neutron scattering experiments. The power-law divergence of the magnetic Grünesien ratio reveals that, surprisingly, this compound is quantum critical without tuning. The dynamical energy over temperature scaling in the neutron response, seen throughout the Brillouin zone, as well as the temperature dependence of the static uniform susceptibility indicate that temperature is the only energy scale in the criticality. Such behavior, which has been associated with Kondo destruction quantum criticality in metallic systems, may well be generic in the semimetal setting.

E-mail: *paschen@ifp.tuwien.ac.at

⊕W.T.F and A.S. contributed equally to this work.

†Present addresses: The Johns Hopkins Applied Physics Laboratory

Quantum criticality is observed in many strongly correlated materials classes, with quantum spin systems[1], high-T_c cuprate[2] and iron pnictide[3] superconductors, and heavy fermion metals[4,5] being prominent examples. Among them, the quantum critical insulators are the best understood. For instance, in the insulating quantum magnet $LiHoF_4$ (Ref. 6), the experimentally detected quantum criticality is well described in terms of the Landau framework, i.e., by the critical fluctuations of the magnetic order parameter[7,8]. In quantum critical metals, by contrast, the underlying physics is much richer. In some systems the Landau description works well[9,10], but in others it appears to fail[5,11]. Theoretically, the charge carriers introduce new couplings to the order parameter or its underlying building blocks, which raises new possibilities for quantum criticality[12–14].

Here we explore the case of the Kondo semimetal $CeRu_4Sn_6$. Its noncentrosymmetric crystal structure (Fig. 1a), strong spin-orbit coupling associated with the three large Z elements, and the fact that the anisotropy in its electronic dispersion[15] cannot be attributed to a nodal ground state wave function of the $Ce^{3+}4f^1$ electron[16] have led to speculations[16] that the material may be topologically nontrivial. Indeed, density functional theory (DFT) calculation within the local density approximation (LDA) plus the Gutzwiller scheme, predict the material to host Weyl nodes[17]. If the nodal excitations persist in a full treatment of the Kondo effect, $CeRu_4Sn_6$ will be a Weyl-Kondo semimetal[18–20]. Our comprehensive investigation of the magnetization, Grüneisen parameter, and inelastic neutron scattering as functions of temperature and magnetic field reveals that this material is quantum critical without tuning, behavior that is only rarely observed[21]. This raises the exciting question as to whether a Weyl-Kondo semimetal phase may indeed be located nearby, nucleating out of the quantum critical fluctuations.

The semimetallic character of $CeRu_4Sn_6$ is evidenced by the weak temperature dependence of the electrical resistivity below about 30 K (Fig. 1b). We have also measured the temperature dependence of the specific heat C_p (Fig. 1c) and the magnetization M, the latter with different magnetic fields H applied along the two main crystallographic directions (perpendicular and parallel to c, Fig. 1d and e, respectively). The high-temperature anisotropy was recently shown to be due to single ion crystal field effects on the $Ce^{3+}4f^1$ electrons[22]. Deviations from this behavior below room temperature indicate a partial gapping of the electronic density of states and/or the onset of Kondo screening[22]. Below 10 K, a strong field dependence is observed. The temperature dependence of the magnetic susceptibility $\chi = M/H|_{10\,\mathrm{mT}}$ is not of simple Curie-Weiss type

[$\chi = C/(T-\Theta)$] but, instead, is well described by

$$\frac{1}{\chi(T)} = \frac{1}{\chi(T=0)} + \frac{(aT)^{\alpha}}{c} \ . \tag{1}$$

with $\alpha = 0.50 \pm 0.01$ and $\alpha = 0.78 \pm 0.03$ for magnetic fields applied perpendicular and parallel to c, respectively (Fig. 1d,e insets). This is inconsistent with quantum criticality involving a Lorentzian fluctuation spectrum, where $\alpha = 1$ (Curie-Weiss law) is expected. The application of larger magnetic fields gradually restores Fermi liquid behavior, i.e., a temperature-independent low-temperature magnetization (Fig. 1d,e main panels).

The magnetic Grüneisen ratio $\Gamma_{\rm mag} = -(\partial M/\partial T)/C_p$ is expected to diverge at any quantum critical point[23], as observed in a number of quantum critical heavy fermion metals[24,25]. For $CeRu_4Sn_6$, from the low-field (10 mT) magnetization and specific heat data presented above, we find $\Gamma_{\rm mag} \sim T^{-\epsilon}$ between about 0.4 and 4 K, with $\epsilon = 1.43 \pm 0.07$ and 1.62 ± 0.11 for fields perpendicular and parallel to the c axis, respectively (Fig. 2a,b), providing strong evidence for quantum criticality without tuning in $CeRu_4Sn_6$.

The field and temperature scaling of the magnetization data underpins this assignment. In Fig. 2c,d we plot $-\partial(M/H)/\partial T \cdot H^{\beta}$ vs T/H^{γ} over more than two orders of magnitude in T/H^{γ}, for fields between 10 mT and 0.5 T both perpendicular and parallel to c. We find a good data collapse with the exponents β being equal to α extracted from Fig. 1d,e (insets) and $\gamma = 0.35 \pm 0.02$ and 0.43 ± 0.02 for fields perpendicular and parallel to c, respectively. The fitted exponents are internally consistent, as they satisfy a scaling relationship (see Supplementary Information). This kind of critical scaling, with a fractional exponent $\alpha < 1$, indicates that the system is at, or very close to, a beyond-Landau quantum critical point, and that magnetic field acts as a tuning parameter, with criticality at $H = 0$.

This is corroborated by our neutron scattering investigation presented next. The inelastic neutron scattering intensity is dominated by features broad in momentum space, with no apparent energy scale, setting the lower bound for a gap in the spin excitations to less than 0.1 meV. In Fig. 3a-c we show the intensity distribution at 1.5 K, integrated from 0.2 meV to 1.2 meV, in the (H0L), (HK0), and (HHL) planes, respectively. The energy profile along two high symmetry directions, (00L) and (H00), integrated over ± 0.2 reciprocal lattice units (r.l.u.) perpendicular to these directions, is presented in Fig. 3d,e. The strong peaks at H+K+L = even are tails of nonmagnetic elastic Bragg scattering. There is no apparent change in the momentum dependence with energy transfer, meaning that the Q and ω dependence of the scattering cross section factorizes

and there is no dispersion. This is clearly at odds with any description of the criticality in terms of the fluctuations of an incipient symmetry-breaking order parameter. The broadness of the features is especially pronounced along $(\frac{1}{2}+\mathrm{H}\,\frac{1}{2}-\mathrm{H}\,0)$ (Fig. 3b) and, to a lesser extent, along the $(\mathrm{H}00)$ direction for peak intensities at $\mathrm{H}+0+\mathrm{L}=\mathrm{odd}$ (Fig. 3a) and symmetry-related directions where the scattering intensity simply follows the magnetic form factor of the $Ce^{3+}4f^1$ electrons. Scattering that is momentum-independent along lines in the Brillouin zone is a sign of local (or Kondo destruction) quantum criticality[12] and has also been observed in quantum critical $CeCu_{5.9}Au_{0.1}$ (Ref. 11). The wavevector dependence of the scattering intensity away from these high-intensity lines is discussed below.

First, however, we investigate whether quantum critical scaling, as evidenced by the static uniform magnetic susceptibility $\chi = (\partial M/\partial H)_{H\to 0} = \chi'(\mathbf{q}=0,\omega=0,T)$ (Fig. 1d,e, insets), is also found in the dynamical spin susceptibility $\chi(\mathbf{q},\omega,T)$. This would give rise to the form

$$\chi(\mathbf{q},\omega,T) = \frac{c}{f(\mathbf{q}) + (-i\hbar\omega + aT)^{\alpha}} \ , \tag{2}$$

where $f(\mathbf{q})$ is an offset and $\alpha = 1$ is expected for a Lorentzian fluctuation spectrum as prescribed by the Landau order parameter description[7,8], and a fractional exponent $\alpha < 1$ points to its failure. The dynamic structure factor $\mathcal{S}(\mathbf{q},\omega,T)$ measured by inelastic neutron scattering is related to the imaginary part of $\chi(\mathbf{q},\omega,T)$ which, near the ordering wave vector, should take the form

$$\chi''(\omega,T) = \frac{1}{T^{\alpha}} \cdot g(\hbar\omega/k_{\mathrm{B}}T) \ . \tag{3}$$

We have determined $\mathcal{S}(\omega,T) \sim \chi''(\omega,T)$ by integrating the neutron scattering intensity for momentum transfers $\mathbf{q}$ about the (100) wavevector, and plot it for temperatures between 0.1 K and 10 K, and energy transfers between 0.1 meV and 1.3 meV as $\mathcal{S}\cdot T^{\alpha}$ vs $\hbar\omega/k_{\mathrm{B}}T$ in Fig. 4a. The best data collapse is found for $\alpha = 0.6 \pm 0.1$ (minimum in χ^2, inset of Fig. 4a). This is consistent with the α values determined from the static uniform magnetic susceptibility ($\alpha = 0.50 \pm 0.01$ for $H \perp c$ and $\alpha = 0.78 \pm 0.03$ for $H \parallel c$), in particular in view of the fact that the neutron scattering intensity is a directional average, taken around the (100) wavevector, where spin fluctuations polarized along and perpendicular to c contribute in equal measures. Thus, also the inelastic neutron scattering data evidence quantum criticality beyond the long-wavelength fluctuations of an order parameter[7,8], such as expected in the theory of Kondo destruction quantum criticality[12].

Finally, we turn to the spatial profile of the critical fluctuations. To do so, we have fitted the the experimental scattering intensity, corrected for the Ce form factor, in terms of Eqn. 2. The

resulting $f(\mathbf{q})$ in the $(\mathrm{H0L})$ and $(\mathrm{HK0})$ planes are shown in Fig. 4b and c, respectively. For the rather featureless $(\frac{1}{2}+\mathrm{H}\,\frac{1}{2}-\mathrm{H}\,0)$ "ridge", the singular dynamical spin susceptibility discussed earlier corresponds to a vanishingly small $f(\mathbf{q})$ (see Fig. 4c). Likewise, in the $(\mathrm{H0L})$ plane, it is seen that $f(\mathbf{q})$ is vanishingly small for $\mathrm{H+0+L}=\mathrm{odd}$, where the dynamical spin susceptibility is also peaked. Along directions that move away from these ridges, the decreasing dynamical spin susceptibility corresponds to an increasing $f(\mathbf{q})$. We can understand these features of $f(\mathbf{q})$ in terms of the wavevector dependence of the Ruderman-Kittel-Kasuya-Yosida (RKKY) interaction

$$J(\mathbf{q}) = J_{\mathrm{K}}^2 L(\mathbf{q}, \omega = 0) = J_{\mathrm{K}}^2 \sum_{\mathbf{k}} \frac{f(\epsilon_{\mathbf{k}}) - f(\epsilon_{\mathbf{k+q}})}{\epsilon_{\mathbf{k+q}} - \epsilon_{\mathbf{k}}} \ . \tag{4}$$

Here, J_{K} is the Kondo coupling strength and $L(\mathbf{q}, \omega)$ the Lindhard function of the (uncorrelated) conduction electrons, which we have determined through LDA-DFT calculations, with one $4f$ electron per Ce^{3+} ion placed in the ionic core. This "f-core" bandstructure, resembling that of $LaRu_4Sn_6$, characterizes the electronic structure of the spd conduction electrons that mediate the RKKY interaction between the $4f$ moments. The associated Fermi surface is shown in Fig. 3f, from which we can identify nesting wavevectors that correspond to the $(\frac{1}{2}+\mathrm{H}\,\frac{1}{2}-\mathrm{H}\,0)$ and $\mathrm{H+0+L}=\mathrm{odd}$ ridges. These can be seen as the broad planes perpendicular to the $(00\mathrm{L})$ direction (Γ to M) and between X points extending along $(00\mathrm{L})$. At these wavevectors, collectively denoted as $\mathbf{Q}$, the RKKY interaction is maximally antiferromagnetic. The Weiss temperature scale

$$\Theta(\mathbf{q}) = J(\mathbf{q}) - J(\mathbf{Q}) \tag{5}$$

provides an understanding of the offset $f(\mathbf{q})$, when the latter is raised to the power $1/\alpha$. In other words, the neutron scattering intensity is maximal where the Weiss temperature $\Theta(\mathbf{q})$ has a minimum, implying that the RKKY interaction defines the $\mathbf{q}$ space structure. Accordingly, the system may be near antiferromagnetic order mediated by the RKKY interaction, with an ordering wavevector at $\mathrm{H+K+L}=\mathrm{odd}$.

Beyond-Landau quantum criticality, as indicated by a fractional exponent $\alpha < 1$, has been documented in a handful of other heavy fermion compounds[11,21,26–28]. Except for the case of the heavy fermion metal $CeCu_{5.9}Au_{0.1}$, a determination of α from inelastic neutron scattering—as provided here—has, however, remained elusive. Our discovery of beyond-Landau quantum criticality, in both the inelastic neutron response and the static uniform magnetic susceptibility, in a genuinely quantum critical semimetal implicates the generality of the phenomenon. Since this constitutes the first observation of this phenomenon in a semimetal, it will be important to

explore whether beyond-Landau quantum criticality is inherent to systems with reduced charge carrier concentration.

In heavy fermion systems, quantum criticality is generally observed at the $T = 0$ collapse of (antiferromagnetically) ordered phases. $CeRu_4Sn_6$, however, is quantum critical without tuning pressure, stoichiometry, or applied fields to a phase boundary. A natural question then arises: Is an antiferromagnetic phase nearby, as suggested by the minima of the Weiss temperature near possible antiferromagnetic ordering wavevectors, and can it be reached by tuning, for instance with pressure? And even more excitingly, do the quantum critical fluctuations give rise to new emergent phases, maybe unconventional superconductivity in analogy to β-$YbAlB_4$ (Ref. 29) or, in view of all the necessary conditions being fulfilled, even a Weyl-Kondo semimetal phase akin to that recently discovered in $Ce_3Bi_4Pd_3$ (refs 18–20)? This will require further experiments at lower temperatures and as function of tuning parameters, which we hope this work will stimulate.

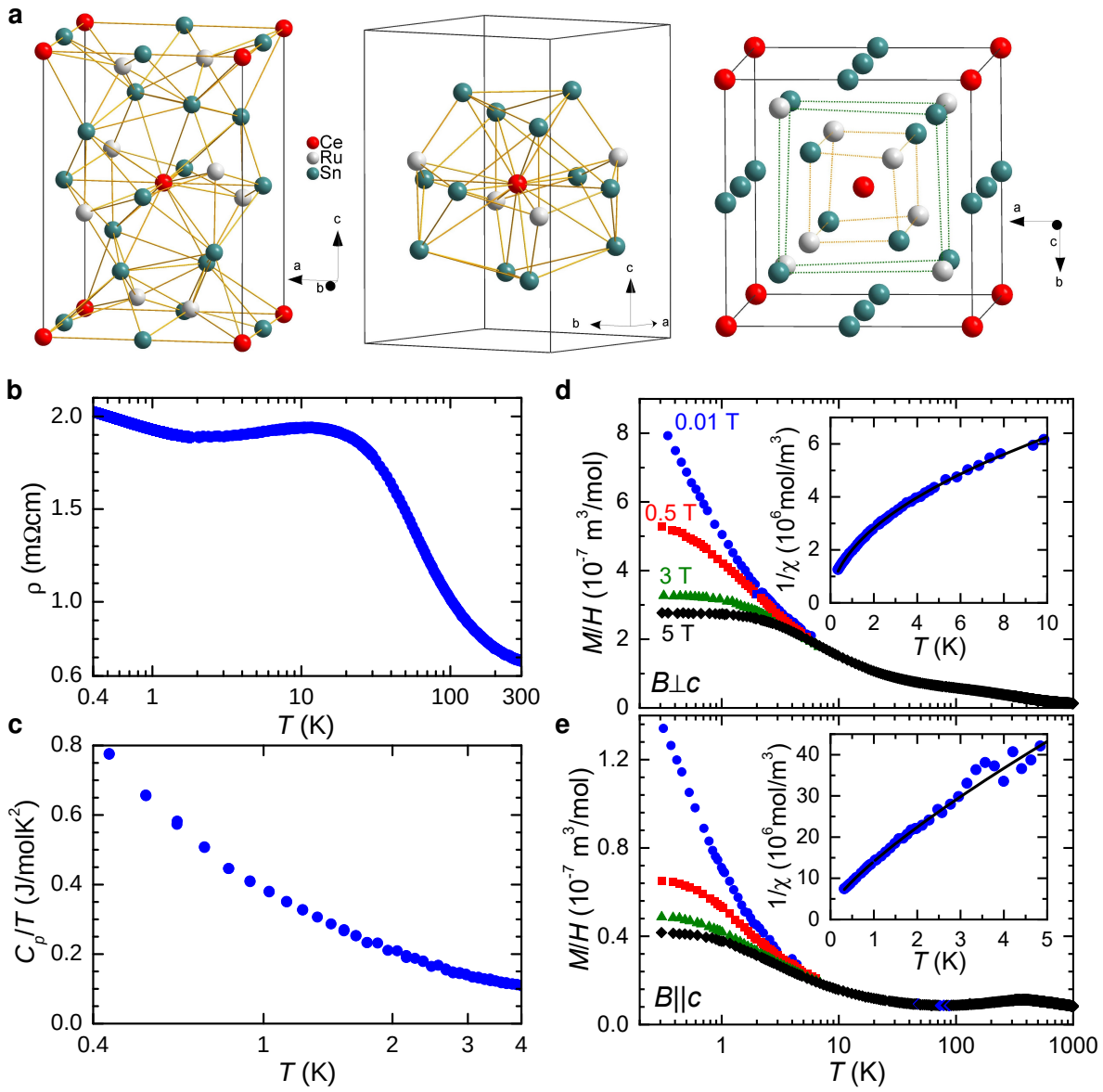

FIG. 1: **Characterization of $CeRu_4Sn_6$.** **(a)** Unit cell with view along tetragonal direction $a = b$ (left), polyhedron around central Ce atom (center), and unit cell with view along c of the noncentrosymmetric tetragonal $I\bar{4}2m$ crystal structure of $CeRu_4Sn_6$, with $a = 6.8810\,\text{Å}$ and $c = 9.7520\,\text{Å}$ (Refs. 30,31). **(b)** Electrical resistivity vs temperature, with current within the tetragonal plane, evidencing the semimetallic character of $CeRu_4Sn_6$. **(c)** Low-temperature specific heat over temperature ratio, plotted on semi-logarithmic scales, evidencing a stronger than logarithmic divergence. **(d)** Magnetization over magnetic field, measured in different magnetic fields ($B = \mu_0 H$) applied perpendicular the tetragonal c axis, as function of temperature. The inset shows the inverse susceptibility, defined as $1/\chi = H/M|_{10\,\text{mT}}$, with a least-square fit with $1/\chi = 1/\chi_0 + c \cdot T^\alpha$ to the date below 10 K, with $\alpha = 0.50 \pm 0.01$. **(e)** Same as **d** for magnetic fields applied along c, with $\alpha = 0.78 \pm 0.03$. The fit was done below 3 K, where the noise in the data is small (note that c is the hard direction, along which χ is much smaller).

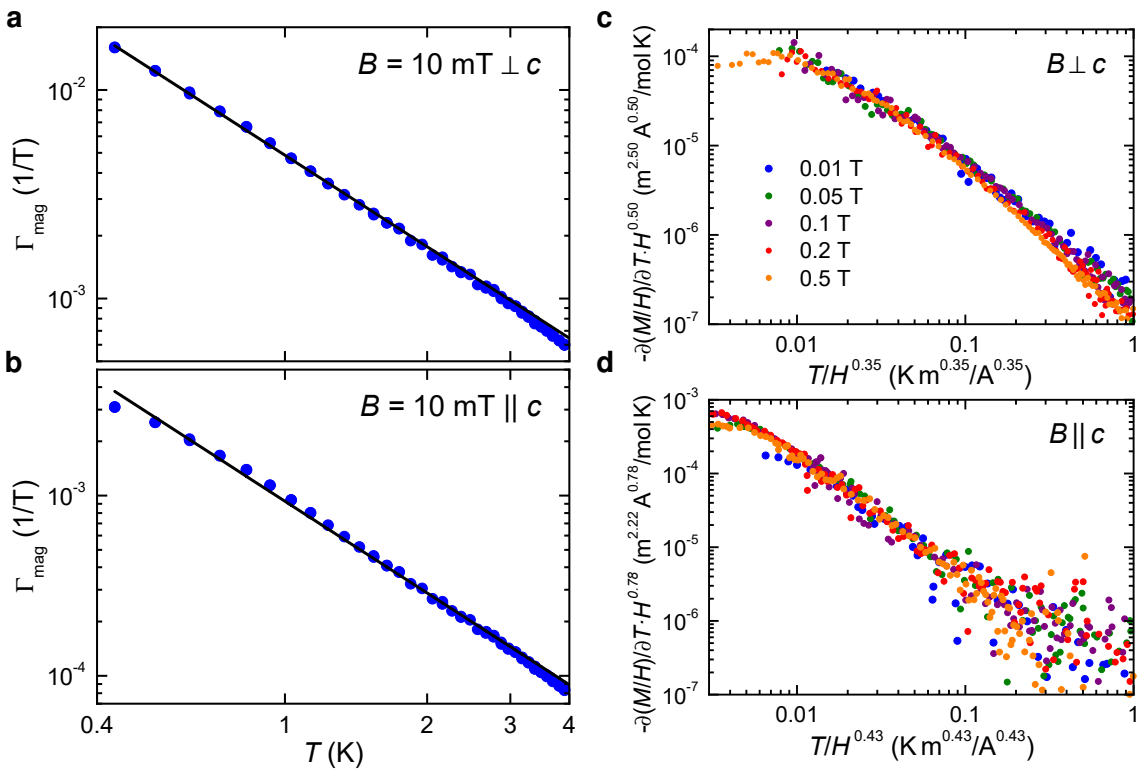

FIG. 2: **Signatures of quantum criticality in thermodynamic properties of $CeRu_4Sn_6$.** **(a)** Magnetic Grüneisen ratio $\Gamma_{\rm mag}$ vs temperature at $B = \mu_0 H = 10\,$mT, applied perpendicular to the c axis, with a power law fit to the data (exponent 1.43 ± 0.07). **(b)** Same as **a** for magnetic fields applied along c, with exponent 1.62 ± 0.11. **(c)** Scaled negative temperature derivative of the magnetization over field ratio, $-\partial(M/H)/\partial T \cdot H^{\beta}$ vs scaled temperature, T/H^{γ}, for fields perpendicular to c, with exponents β and γ that collapse the data. **(d)** Same as **c** for magnetic fields applied along c.

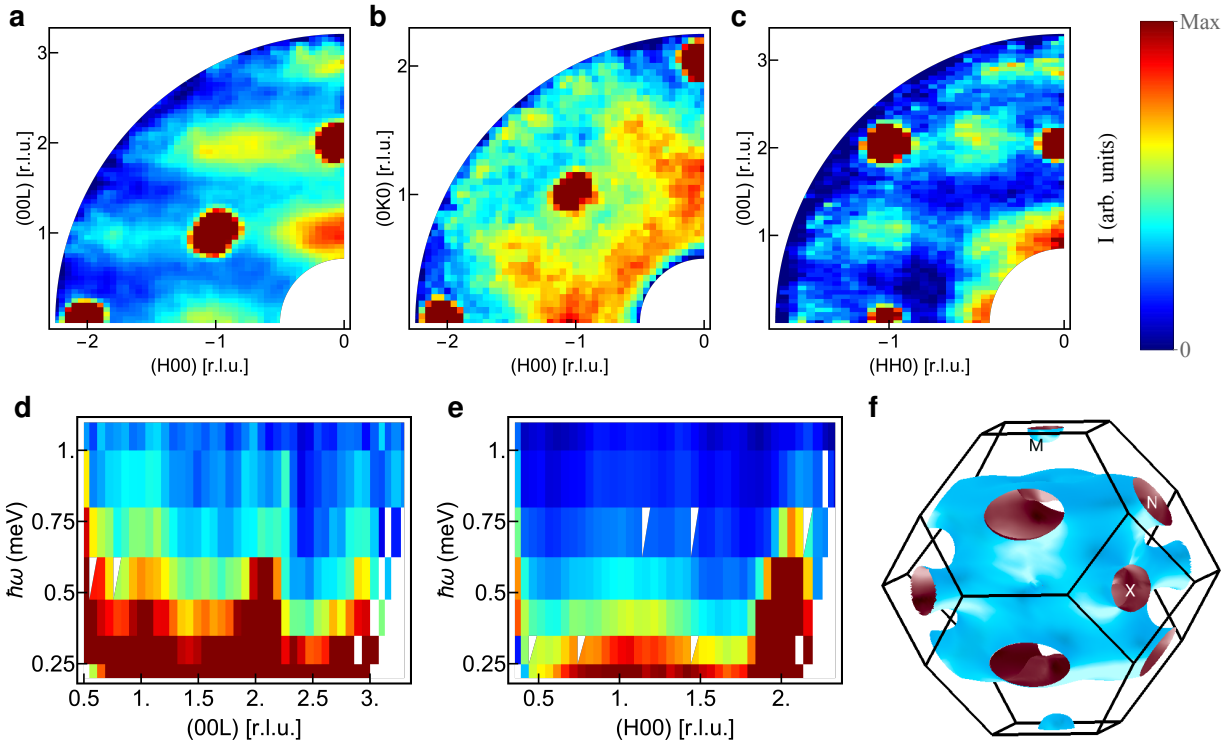

FIG. 3: **Quasielastic neutron scattering from $CeRu_4Sn_6$. (a,b,c)** Energy integrated neutron scattering intensity in the $(\mathrm{H0L})$, $(\mathrm{HK0})$, and (HHL) planes, respectively. Saturated intensity at $\mathrm{H{+}K{+}L = even}$ is residual Bragg intensity. Along $(\frac{1}{2}{+}\mathrm{H}\,\frac{1}{2}{-}\mathrm{H}\,0)$ and equivalent directions in **b** and, to a lesser extent, along $(\mathrm{H00})$ centered at $\mathrm{H{+}0{+}L = odd}$ in **a** the scattering intensity is almost structureless. **(d,e)** Energy vs momentum along $(\mathrm{00L})$ and $(\mathrm{H00})$, respectively. The Q and ω dependence of the scattering cross section factorizes so that there is no dispersion and the signal continues below the resolution limit of the instrument. **(f)** "f-core" Fermi surface derived from LDA-DFT calculations.

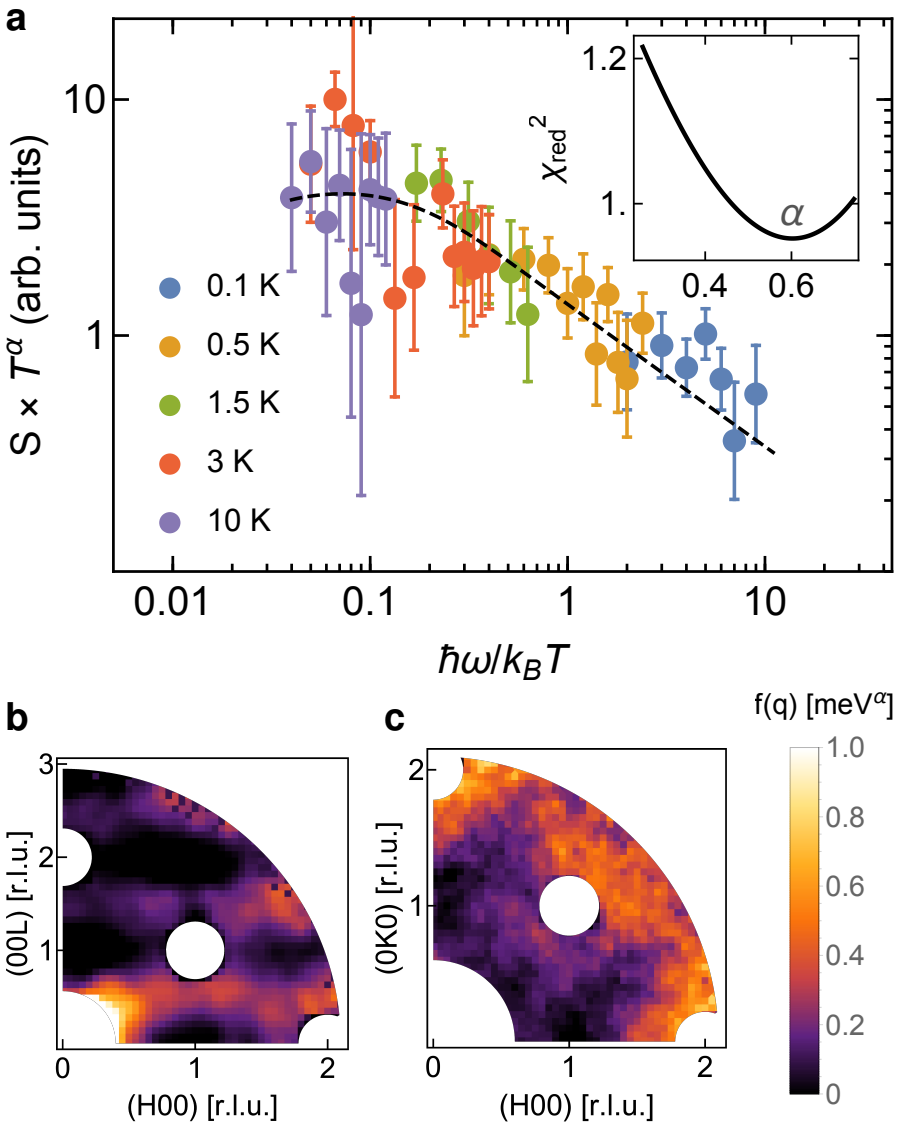

FIG. 4: **Dynamical scaling of $CeRu_4Sn_6$. (a)** Scaled neutron scattering intensity, $\mathcal{S} \cdot T^{\alpha}$, vs scaled energy transfer, $\hbar\omega/k_{\mathrm{B}}T$. The inset shows the scaled χ^2_{red}, which is minimal for $\alpha = 0.6$. **(b,c)** $f(\mathbf{q})$ (see Eqn. 2) in the $(\mathrm{H0L})$ and $(\mathrm{HK0})$ plane, respectively, obtained through a global fit of Eqn. 2 to the q-E dependent data in Fig. 3 with a single consistent value of α. The white areas correspond to blinded out data near the nuclear Bragg peaks, which are situated at H+K+L = even. Along $(\frac{1}{2}+\mathrm{H}\ \frac{1}{2}-\mathrm{H}\ 0)$ in **c** and about $(\mathrm{H}01)$ in **b**, $f(\mathbf{q})$ is minimal, indicating maximally antiferromagnetic interactions (see text).

Methods

For our study, single crystals of $CeRu_4Sn_6$ were grown from self-flux, using the floating zone melting technique with optical heating as reported previously[32]. The magnetic properties between 2 K and 300 K were measured in a SQUID magnetometer from Cryogenic Ltd., the data between 0.3 K and 2 K employed a ^{3}He insert. High-temperature magnetization measurements up to 1000 K were performed with a vibrating sample magnetometer in a PPMS from Quantum Design. The ^{3}He PPMS option was used for specific heat measurements in the temperature range from 0.3 K to 20 K.

Neutron scattering was performed with the MACS spectrometer at the NIST NCNR. For the momentum-space mapping, we co-aligned 3 g of single crystals and used incident energies from 3.7 meV to 5 meV and a fixed final energy of 3.7 meV, allowing for the use of Be and BeO filters before and after the sample, respectively, and providing an effective resolution better than 0.05 Å^{-1} and 0.15 meV. For the ω/T scaling measurements, 2 g of single crystals were accommodated within the restrictions of a dilution refrigerator. We utilized a fixed final energy of 2.5 meV and incident energies up to 3.7 meV. A magnetic field of 10 mT was applied along $(0\mathrm{K}0)$ to avoid superconductivity in the aluminum sample mount and maintain good thermal contact.

Acknowledgements

The work at IQM was supported as part of the Institute for Quantum Matter, an Energy Frontier Research Center funded by the U.S. Department of Energy, Office of Science, Basic Energy Sciences under Award No. de-sc0019331. CB was supported by the Gordon and Betty Moore Foundation through GBMF-4532. S.P. and A.S. acknowledge financial support from the European Community (H2020 Project No. 824109) and from the Austrian Science Fund (FWF projects P29296-N27, 29279-N27, and W1243). Q.S. was supported by the NSF (Grant No. DMR-1920740) and the Robert A. Welch Foundation (Grant No. C-1411), and acknowledges the hospitality of the Aspen Center for Physics, which is supported by the NSF (Grant No. PHY-1607611). WTF is grateful to the ARCS foundation, Lockheed Martin and KPMG for the partial support of this work and to Predrag Nikolic for fruitful discussions.

1. Coldea, R., Tennant, D. A., Wheeler, E. M., Wawrzynska, E., Prabhakaran, D., Telling, M., Habicht, K., Smeibidl, P. & Kiefer, K. Quantum criticality in an Ising chain: Experimental evidence for emergent E_8 symmetry. *Science* **327**, 177 (2010).
2. Sachdev, S. Where is the quantum critical point in the cuprate superconductors? *Phys. Status Solidi B* **247**, 537 (2010).
3. Dai, J., Si, Q., Zhu, J.-X. & Abrahams, E. Iron pnictides as a new setting for quantum criticality. *Proc. Natl. Acad. Sci. U.S.A.* **106**, 4118 (2009).
4. v. Löhneysen, H., Rosch, A., Vojta, M. & Wölfle, P. Fermi-liquid instabilities at magnetic quantum critical points. *Rev. Mod. Phys.* **79**, 1015 (2007).
5. Kirchner, S., Paschen, S., Chen, Q., Wirth, S., Feng, D., Thompson, J. D. & Si, Q. Colloquium: Heavy-electron quantum criticality and single-particle spectroscopy. *Rev. Mod. Phys.* **92**, 011002 (2020).
6. Bitko, D., Rosenbaum, T. F. & Aeppli, G. Quantum critical behavior for a model magnet. *Phys. Rev. Lett.* **77**, 940 (1996).
7. Hertz, J. A. Quantum critical phenomena. *Phys. Rev. B* **14**, 1165 (1976).
8. Millis, A. J. Effect of a nonzero temperature on quantum critical points in itinerant fermion systems. *Phys. Rev. B* **48**, 7183 (1993).
9. Küchler, R., Oeschler, N., Gegenwart, P., Cichorek, T., Neumaier, K., Tegus, O., Geibel, C., Mydosh, J. A., Steglich, F., Zhu, L. & Si, Q. Divergence of the Grüneisen ratio at quantum critical points in heavy fermion metals. *Phys. Rev. Lett.* **91**, 066405 (2003).
10. Jaramillo, R., Feng, Y., Wang, J. & Rosenbaum, T. F. Signatures of quantum criticality in pure Cr at high pressure. *Proc. Natl. Acad. Sci. U.S.A.* **107**, 13631 (2010).
11. Schröder, A., Aeppli, G., Coldea, R., Adams, M., Stockert, O., v. Löhneysen, H., Bucher, E., Ramazashvili, R. & Coleman, P. Onset of antiferromagnetism in heavy-fermion metals. *Nature* **407**, 351 (2000).
12. Si, Q., Rabello, S., Ingersent, K. & Smith, J. Locally critical quantum phase transitions in strongly correlated metals. *Nature* **413**, 804 (2001).
13. Lee, S.-S. Low-energy effective theory of Fermi surface coupled with U(1) gauge field in $2+1$ dimensions. *Phys. Rev. B* **80**, 165102 (2009).
14. Mross, D. F., McGreevy, J., Liu, H. & Senthil, T. Controlled expansion for certain non-Fermi-liquid

metals. *Phys. Rev. B* **82**, 045121 (2010).

15. Guritanu, V., Wissgott, P., Weig, T., Winkler, H., Sichelschmidt, J., Scheffler, M., Prokofiev, A., Kimura, S., Iizuka, T., Strydom, A. M., Dressel, M., Steglich, F., Held, K. & Paschen, S. Anisotropic optical conductivity of the putative Kondo insulator $CeRu_4Sn_6$. *Phys. Rev. B* **87**, 115129 (2013).
16. Sundermann, M., Strigari, F., Willers, T., Winkler, H., Prokofiev, A., Ablett, J. M., Rueff, J. P., Schmitz, D., Weschke, E., Moretti Sala, M., Al-Zein, A., Tanaka, A., Haverkort, M. W., Kasinathan, D., Tjeng, L. H., Paschen, S. & Severing, A. $CeRu_4Sn_6$: a strongly correlated material with nontrivial topology. *Sci. Rep.* **5**, 17937 (2015).
17. Xu, Y., Yue, C., Weng, H. & Dai, X. Heavy Weyl fermion state in $CeRu_4Sn_6$. *Phys. Rev. X* **7**, 011027 (2017).
18. Dzsaber, S., Prochaska, L., Sidorenko, A., Eguchi, G., Svagera, R., Waas, M., Prokofiev, A., Si, Q. & Paschen, S. Kondo insulator to semimetal transformation tuned by spin-orbit coupling. *Phys. Rev. Lett.* **118**, 246601 (2017).
19. Lai, H.-H., Grefe, S. E., Paschen, S. & Si, Q. Weyl-Kondo semimetal in heavy-fermion systems. *Proc. Natl. Acad. Sci. U.S.A.* **115**, 93 (2018).
20. Dzsaber, S., Yan, X., Eguchi, G., Prokofiev, A., Shiroka, T., Blaha, P., Rubel, O., Grefe, S. E., Lai, H.-H., Si, Q. & Paschen, S. Giant spontaneous Hall effect in a nonmagnetic Weyl-Kondo semimetal. *arXiv:1811.02819* (2018).
21. Matsumoto, Y., Nakatsuji, S., Kuga, K., Karaki, Y., Horie, N., Shimura, Y., Sakakibara, T., Nevidomskyy, A. H. & Coleman, P. Quantum criticality without tuning in the mixed valence compound β-$YbAlB_4$. *Science* **331**, 316 (2011).
22. Amorese, A., Kummer, K., Brookes, N. B., Stockert, O., Adroja, D. T., Strydom, A. M., Sidorenko, A., Winkler, H., Zocco, D. A., Prokofiev, A., Paschen, S., Haverkort, M. W., Tjeng, L. H. & Severing, A. Determining the local low-energy excitations in the Kondo semimetal $CeRu_4Sn_6$ using resonant inelastic x-ray scattering. *Phys. Rev. B* **98**, 081116 (2018).
23. Zhu, L., Garst, M., Rosch, A. & Si, Q. Universally diverging Grüneisen parameter and the magnetocaloric effect close to quantum critical points. *Phys. Rev. Lett.* **91**, 066404 (2003).
24. Tokiwa, Y., Radu, T., Geibel, C., Steglich, F. & Gegenwart, P. Divergence of the magnetic Grüneisen ratio at the field-induced quantum critical point in $YbRh_2Si_2$. *Phys. Rev. Lett.* **102**, 066401 (2009).
25. Gegenwart, P. Grüneisen parameter studies on heavy fermion quantum criticality. *Rep. Prog. Phys.* **79**, 114502 (2016).

26. Ishida, K., Okamoto, K., Kawasaki, Y., Kitaoka, Y., Trovarelli, O., Geibel, C. & Steglich, F. $YbRh_2Si_2$: Spin fluctuations in the vicinity of a quantum critical point at low magnetic fields. *Phys. Rev. Lett.* **89**, 107202 (2002).

27. Baumbach, R., Ho, P., Sayles, T., Maple, M., Wawryk, R., Cichorek, T., Pietraszko, A. & Henkie, Z. Non-Fermi-liquid behavior in the filled skutterudite compound $CeRu_4As_{12}$. *J. Phys.: Condens. Matter* **20**, 075110 (2008).

28. Bauer, E., Slebarski, A., Dickey, R., Freeman, E., Sirvent, C., Zapf, V., Dilley, N. & Maple, M. Electronic and magnetic investigation of the filled skutterudite compound $CeRu_4Sb_{12}$. *J. Phys.: Condens. Matter* **13**, 5183 (2001).

29. Nakatsuji, S., Kuga, K., Machida, Y., Tayama, T., Sakakibara, T., Karaki, Y., Ishimoto, H., Yonezawa, S., Maeno, Y., Pearson, E., Lonzarich, G., Balicas, L., Lee, H. & Fisk, Z. Superconductivity and quantum criticality in the heavy-fermion system β-$YbAlB_4$. *Nature Phys.* **4**, 603 (2008).

30. Venturini, G., Chafik El Idrissi, B., Marêché, J. F. & Malaman, B. . *Mater. Res. Bull.* **25**, 1541 (1990).

31. Das, I. & Sampathkumaran, E. V. Electrical-resistance anomalies in the Ce-Ru-Sn phase. *Phys. Rev. B* **46**, 4250 (1992).

32. Paschen, S., Winkler, H., Nezu, T., Kriegisch, M., Hilscher, G., Custers, J., Prokofiev, A. & Strydom, A. Anisotropy of the Kondo insulator $CeRu_4Sn_6$. *J. Phys. Conf. Series* **200**, 012156 (2010).

33. Shirane, G., Shapiro, S. M. & Tranquada, J. M. *Neutron Scattering with a Triple-Axis Spectrometer* (Cambridge Univ. Press, Cambridge, 2002).

34. Xu, G., DiTusa, J. F., Ito, T., Oka, K., Takagi, H., Broholm, C. & Aeppli, G. Y_2BaNiO_5: A nearly ideal realization of the $S = 1$ Heisenberg chain with antiferromagnetic interactions. *Phys. Rev. B* **54**, R6827 (1996).

Supplementary Information

Scaling and exponent relationship

Here we derive a relationship between the scaling exponents, which we first summarize. The exponent α characterizes the temperature dependence of the magnetization, and is defined as the exponent in the power-law temperature dependence of the linear-response magnetic susceptibility

$$\chi(T) \sim \frac{1}{T^{\alpha}} \,. \tag{6}$$

We also introduce β and γ, which describe the magnetic-field dependence of the nonlinear magnetization. The exponent γ is defined by generalizing Eqn. 6 to the case when the magnetic field is not vanishingly small, namely by

$$\frac{M}{H} = \frac{1}{T^{\alpha}} f(T/H^{\gamma}) \tag{7}$$

which, when taking the limit $H \to 0$, recovers Eqn. 6. Additionally, the exponent β is defined through the scaling of the temperature derivative of the magnetization as

$$\frac{\partial(M/H)}{\partial T} \times H^{\beta} = g(T/H^{\gamma}) \,. \tag{8}$$

Based on scaling (dimensional analysis), Eqn. 7 implies that

$$\frac{\partial(M/H)}{\partial T} = \frac{1}{T^{1+\alpha}} f_1(T/H^{\gamma}) \,, \tag{9}$$

which is equivalent to

$$\frac{\partial(M/H)}{\partial T} = \frac{1}{H^{\gamma(1+\alpha)}} g(T/H^{\gamma}) \,. \tag{10}$$

Comparing Eqs. 8 and 10 gives rise to the relationship

$$\beta = \gamma(1+\alpha) \tag{11}$$

among the three exponents.

We now apply this relationship to the exponents we have extracted for $CeRu_4Sn_6$. Consider first $H \perp c$. The fitted exponents are $\alpha = 0.5$, $\gamma = 0.35$, and $\beta = 0.5$. The product $\gamma(1+\alpha) = 0.525$ is compatible with β within about 5% (thus within the experimental error bars, see main text). For $H \parallel c$, the fitted exponents are $\alpha = 0.78$, $\gamma = 0.43$, and $\beta = 0.78$. The product $\gamma(1+\alpha) = 0.765$ is consistent with β within about 2%, again within experimental accuracy.

We note that we have assumed hyperscaling in the derivation of the scaling relationship[23]. The hyperscaling is expected to be satisfied at interacting critical points. By contrast, Gaussian critical

points will contain dangerously irrelevant variables that may invalidate the hyperscaling for some observables. The fact that the fitted exponents obey the scaling relationship is consistent with the interacting nature of the quantum critical point that underlies the observations reported in the present work for $CeRu_4Sn_6$.

Neutron Scattering

Background from the sample environment was accounted for by subtraction of a linear combination of separate measurements of count rates for an empty sample can and a CYTOP-only standard (CYTOP is a fluorine-based epoxy that we used to secure the $CeRu_4Sn_6$ single crystals).

For incident energies below 3.7 meV, neutrons are incapable of undergoing Bragg diffraction with Al in and around the beam path, dramatically reducing the background associated with Bragg scattering from the split-coil magnet system.

Sample-out background scattering was subtracted to remove contamination at low scattering angles. To account for incoherent elastic nuclear scattering from the sample, a pseudovoigt function was fit to the high-Q incoherent elastic profile and scaled to the elastic line intensity with same magnitude of Q as where our E/T scaling fit was performed, at a point in the Brillouin zone where magnetic intensity is at a minimum. The data for E/T scaling was collected at (100), and integrated ± 0.2 r.l.u. along $(\mathrm{H}00)$ and $(00\mathrm{L})$.

The modulation in intensity outside of the first zone by translation of a reciprocal lattice vector provides information on the microscopic origin of the scattering. The magnetic form factor, F_{mag}, modulates scattering intensity as $I(\boldsymbol{q}+\boldsymbol{G}) = I(\boldsymbol{q}) \cdot |F_{\mathrm{mag}}(\boldsymbol{q}+\boldsymbol{G})|^2$ (Ref. 33). The response of unpolarized neutrons is then described by a linear combination of the components of the dynamic spin correlation function[34] as

$$I(\mathbf{Q},\omega) = \sin^2\theta \cdot \mathcal{S}^{aa}(\mathbf{Q},\omega) + (1-\sin^2\theta\cos^2\phi)\mathcal{S}^{bb}(\mathbf{Q},\omega) + (1-\sin^2\theta\sin^2\theta)\mathcal{S}^{cc}(\mathbf{Q},\omega)\ . \quad (12)$$

We find that $\mathcal{S}^{aa} = \mathcal{S}^{bb} = 2\mathcal{S}^{cc}$ improves the correspondence with the observed intensity modulation. This modulation effectively accounts for a magnetic form factor which is the result of anisotropic hybridization and/or easy plane crystal field anisotropy. Previous field-dependent heat capacity measurements show a field-induced extra contribution below about 10 K, that is much larger for $H \perp c$ than for $H \parallel c$ (Ref. 32), consistent with our observation of a form factor and polarization factor which implies quasielastic fluctuations of easy-plane Ce $4f$ electrons at low temperatures.